PHYSICAL REVIEW A **67**, 011401(R) (2003)

Magnetic trapping of metastable $^3P_2$ atomic strontium

S. B. Nagel, C. E. Simien, S. Laha, P. Gupta, V. S. Ashoka, and T. C. Killian
Department of Physics and Astronomy and Rice Quantum Institute, Rice University, Houston, Texas 77251
(Received 17 September 2002; published 13 January 2003)

We report the magnetic trapping of metastable $^3P_2$ atomic strontium. Atoms are cooled in a magneto-optical trap (MOT) operating on the dipole-allowed $^1S_0$-$^1P_1$ transition at 461 nm. Decay via $^1P_1 \rightarrow {}^1D_2 \rightarrow {}^3P_2$ continuously loads a magnetic trap formed by the quadrupole magnetic field of the MOT. Over 10^8 atoms at a density of 8×10^9 cm^{-3} and temperature of 1 mK are trapped. The atom temperature is significantly lower than what would be expected from the kinetic and potential energies of atoms as they are transferred from the MOT. This suggests the occurrence of thermalization and evaporative cooling in the magnetic trap.

DOI: 10.1103/PhysRevA.67.011401 PACS number(s): 32.80.Pj

Laser-cooled alkaline-earth-metal atoms offer many possibilities for practical applications and fundamental studies. The two valence electrons in these systems give rise to triplet and singlet levels connected by narrow intercombination lines that are utilized for optical frequency standards [1]. Laser cooling on such a transition in strontium may lead to a fast and efficient route to all-optical quantum degeneracy [2,3], and there are abundant bosonic and fermionic isotopes for use in this pursuit. The lack of hyperfine structure in the bosonic isotopes and the closed electronic shell in the ground states make alkaline-earth-metal atoms appealing testing grounds for cold-collision theories [4–6], and collisions between metastable alkaline-earth-metal atoms is a relatively new and unexplored area for research [7].

In this paper we characterize a technique that should benefit all these experiments—the continuous loading of metastable $^3P_2$ atomic strontium (^{88}Sr) from a magneto-optical trap (MOT) into a purely magnetic trap. This idea was discussed in a recent theoretical study of alkaline-earth-metal atoms and ytterbium [8]. Katori *et al.* [9] and Loftus *et al.* [10] have also reported observing this phenomenon in their strontium laser-cooling experiments. Continuous loading of a magnetic trap from a MOT was recently described for chromium atoms [11].

This scheme should allow for collection of large numbers of atoms at high density since atoms are shelved in a dark state and are less susceptible to light-assisted collisional loss mechanisms [4,6,12]. It is an ideal starting place for many experiments such as sub-Doppler laser cooling on a transition from the metastable state, as has been done with calcium [13], production of ultracold Rydberg gases [14] or plasmas [15], and evaporative cooling to quantum degeneracy. Optical frequency standards based on laser-cooled alkaline-earth-metal atoms, which are currently limited by high sample temperatures [1], may benefit from the ability to trap larger numbers of atoms and evaporatively cool them in a magnetic trap.

We will first describe the operation of the Sr MOT and how this loads the magnetic trap with $^3P_2$ atoms. Then we will characterize the loading and decay rates of atoms in the magnetic trap. Finally, we will present measurements of the $^3P_2$ sample temperature.

Sr atoms are loaded from a Zeeman-slowed atomic beam [16] and cooled and trapped in a standard MOT [17]. Both operate on the 461-nm $^1S_0$-$^1P_1$ transition (Fig. 1). Blue light is generated by frequency doubling the output of a Ti:sapphire laser using $KNbO_3$ in two external buildup cavities [18]. 150 mW of power, red detuned from resonance by 585 MHz, is available for the Zeeman slower. Three beams of about 1 cm diameter, each with intensity $I \leqslant I_{sat} = 45$ mW/cm^2, and 57 MHz red detuned, are sent to the apparatus and retroreflected to produce the 6-beam MOT.

The 30-cm-long Zeeman slower connects a vacuum chamber for the Sr oven and nozzle to the MOT chamber. Each chamber is evacuated by a 75 l/s ion pump. When the Sr oven is operated at its normal temperature of about 550 °C, the pressure in the MOT chamber is about 5×10^{-9} torr, and the oven chamber is at 4×10^{-8} torr.

Extended cavity diode lasers at 679 and 707 nm remove population from the $^3P_0$ and $^3P_2$ levels. Each laser provides several hundred microwatts of power and is locked to an absorption feature in a discharge cell. These are not used for the operation of the MOT during experiments with $^3P_2$ atoms. They serve to repump atoms from the $^3P_2$ level to the ground state via the $^3S_1$ and $^3P_1$ levels for imaging diagnostics.

The quadrupole magnetic field for the MOT is produced by flowing up to 80 A of current in opposite directions through two coils of 36 turns each, with coil diameter of 4.3 cm and separation of 7.7 cm. The maximum current produces a field gradient along the symmetry axis of the coils of 115 G/cm. Such a large field gradient, about ten times the norm for an alkali-metal atom MOT, is required because of

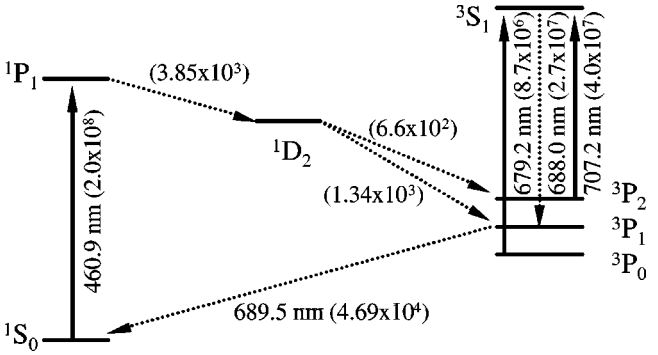

FIG. 1. Strontium energy levels involved in the trapping of $^3P_2$ atoms. Decay rates (s^{-1}) and selected excitation wavelengths are given. Laser light used for the experiment is indicated by solid lines.

the large decay rate of the excited state ($\Gamma_{^1P_1}=2\pi \times 32$ MHz) and the comparatively large recoil momentum of 461 nm photons.

Typically 10^7–10^8 atoms are held in the MOT, at a peak density of $n\approx 1\times 10^{10}$ cm^{-3}, with an rms radius of 1.2 mm and temperatures from 2 to 10 mK. The cooling limit for the MOT is the Doppler limit ($T_{Doppler}=0.77$ mK) because the ground state lacks degeneracy and thus cannot support sub-Doppler cooling. Higher MOT laser power produces not only higher MOT temperature, but also a larger number of trapped atoms. These sample parameters are measured with absorption imaging of a near resonant probe beam. The temperature is determined by monitoring the velocity of ballistic expansion of the atom cloud [19] after the trap is extinguished.

Atoms escape from the MOT due to $^1P_1$–$^1D_2$ decay as discussed in Ref. [8]. From the $^1D_2$ state atoms either decay to the $^3P_1$ state and then to the ground state and are recaptured in the MOT, or they decay to the $^3P_2$ state, which has a lifetime of 17 min [7]. The decay rates are given in Fig. 1. The resulting MOT lifetime of 11–55 ms was measured by turning off the Zeeman-slowing laser beam and by monitoring the decay of the MOT fluorescence. The lifetime is inversely proportional to the fraction of time atoms spend in the $^1P_1$ level, which varies with MOT laser power. Light-assisted collisional losses from the MOT [6] are negligible compared to the rapid $^1P_1$-$^1D_2$ decay.

The $m_j=2$ and $m_j=1$ $^3P_2$ states can be trapped in the MOT quadrupole magnetic field. Such a quadrupole magnetic trap was used for the first demonstration of magnetic trapping of neutral atoms [20], but in that case atoms were loaded directly from a Zeeman-slowed atomic beam.

Near the center of the trap, the magnetic interaction energy for $^3P_2$ atoms takes the form

$$U_{m_j}=-\boldsymbol{\mu}_{m_j}\cdot\mathbf{B}=g\mu_B m_j b\sqrt{x^2/4+y^2+z^2/4}, \qquad (1)$$

where m_j is the angular-momentum projection along the local field, $g=3/2$ is the g factor for the $^3P_2$ state, μ_B is the Bohr magneton, and $b\leqslant 115$ G/cm is the gradient of the magnetic field along the symmetry (y) axis of the quadrupole coil. For the $m_j=2$ state and the maximum b, $g\mu_B m_j/k_B=200$ μK/G and the barrier height for escape from the center of the magnetic trap is 15 mK. Gravity, which is oriented along z, corresponds to an effective field gradient of only 5 G/cm for Sr and is neglected in our analysis.

Typical data showing the magnetic trapping are shown in Fig. 2. We are unable to directly image atoms in the $^3P_2$ state, so we use the 679 and 707 nm lasers to repump them to the ground state for fluorescence detection on the $^1S_0$-$^1P_1$ transition. The details are as follows. The MOT is operated for $t_{load}\leqslant 1300$ ms, during this time atoms continuously load the magnetic trap. The MOT and Zeeman slower light is then extinguished, and after a time t_{hold}, the MOT lasers and repump laser at 707 nm are turned on. The 679 nm laser is left on throughout. Any atoms in the $^3P_2$ state are cycled through the $^3P_1$ level to the ground state within 500 μs of repumping, and they fluoresce in the field of the MOT lasers. If the magnetic field is not left on during t_{hold}, Fig. 2 shows

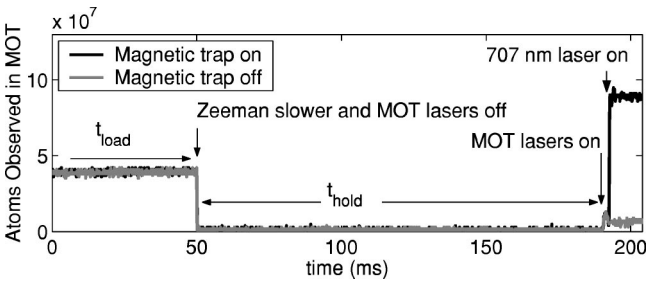

FIG. 2. Magnetic trapping of $^3P_2$ atoms. Ground-state atoms are detected by fluorescence from the MOT lasers. If the quadrupole magnetic field is left on during t_{hold} (black trace), large numbers of $^3P_2$ atoms are magnetically trapped until the 707 nm laser returns them to the ground state. The residual fluorescence after t_{hold} for the gray trace arises from background scatter off atoms in the atomic beam. Reloading of the MOT from the atomic beam is negligible with the Zeeman slower light blocked. There is a 1-ms delay between the MOT and 707 nm laser turn on to allow the MOT light intensity to reach a stable value.

that a negligible number of ground-state atoms are present in the MOT when the lasers are turned on. If the magnets are left on, however, the MOT fluorescence shows that $^3P_2$ atoms were held in the magnetic trap.

The maximum number of $^3P_2$ atoms trapped is about 1×10^8, and the peak density is about 8×10^9 cm^{-3}. To determine what limits this number, we varied t_{hold} and saw that the number of $^3P_2$ atoms varied as $N_0 e^{-\gamma t_{\rm hold}}$. The fits were excellent and the decay rate was proportional to background pressure as shown in Fig. 3(a). This implies that for our conditions, the trap lifetime is limited by collisions with residual background gas molecules, and strontium-strontium collisional losses are not a dominant effect.

The magnetic trap loading rate was determined by holding t_{hold} constant and varying t_{load}. The loading rate correlates with the atom loss rate from the MOT [Fig. 3(b)]. At low MOT loss rates, about 10% of the atoms lost from the MOT are captured in the magnetic trap. From the Clebsch-Gordon coefficients involved in atom decay from the $^1P_1$ state, and the magnetic sublevel distribution for atoms in the MOT, one expects that about 25% of the atoms decaying to $^3P_2$ enter the $m_j=1$ or $m_j=2$ states. This is significantly higher than the largest observed efficiencies, and we may be seeing signs of other processes, such as losses due to collisions with MOT atoms. This phenomenon dominated dynamics during the loading of a magnetic trap from a chromium MOT [11].

At larger MOT loss rates (corresponding to higher MOT laser intensities, MOT temperatures, and trapped $^3P_2$ atom densities), the efficiency of loading the magnetic trap decreases by about a factor of 2. MOT temperatures approach the trap depth for the largest loading rates and we attribute the decreasing efficiency to the escape of atoms over the magnetic barrier.

The 500 μs required for repumping is fast compared to the time scale for the motion of the atoms, so absorption images of ground-state atoms immediately after repumping provide a measure of the density distribution of the magnetically trapped sample. For these measurements, the magnetic trap is loaded for 1.3 s. Then the magnetic field is turned off

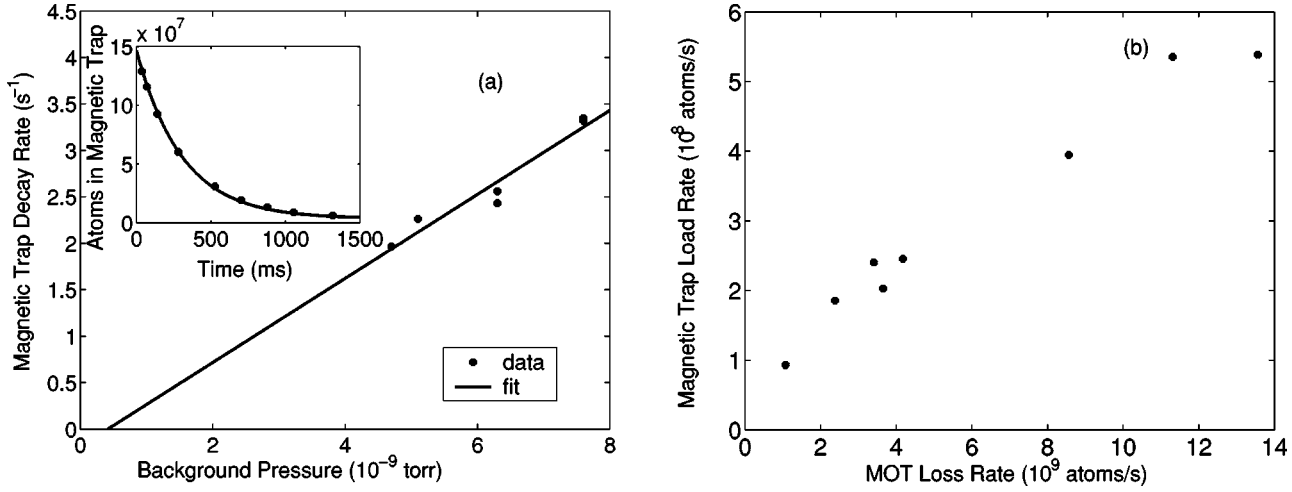

FIG. 3. (a) The lifetime of atoms in the magnetic trap is limited by collisions with background gas molecules. The linear fit extrapolates to zero at zero pressure within statistical uncertainties. Inset: a typical fit of the decay of the number of trapped atoms to a single exponential. (b) The magnetic trap loading rate is plotted against the MOT loss rate. Data correspond to various MOT laser powers and slow-atom fluxes from the atomic beam.

and the repump lasers are turned on. After 500 μs, an 80-μs pulse of a weak 461 nm probe beam ($I \ll I_{sat}$), 12.5 MHz detuned below resonance, illuminates the atom cloud and falls on a charge-coupled device camera. We record an intensity pattern when atoms are present, $I(x,y)_{atoms}$, and a background pattern when no atoms are present, $I(x,y)_{back}$. To analyze the data, we plot (Fig. 4)

$$S(x) = \int_{image} dy \ln[I(x,y)_{back}/I(x,y)_{atoms}]$$

$$= \sigma_{abs} \int_{image} dy \int_{-\infty}^{\infty} dz n(x,y,z), \qquad (2)$$

and the analogously defined $S(y)$, where σ_{abs} is the absorption cross section and $n(x,y,z)$ is the atom density. Because we do not know the distribution of magnetic sublevels, we make the simplifying assumption that all atoms are in the $m_j = 2$ state, and the density is given by

$$n(x,y,z) = n_0 \exp[-U_2(x,y,z)/k_B T]. \qquad (3)$$

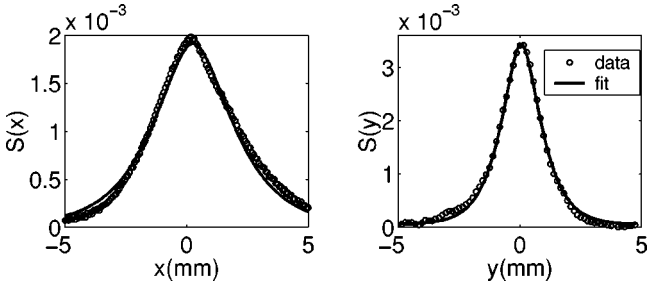

FIG. 4. Distributions of $^3P_2$ atoms extracted from absorption images of ground-state atoms shortly after repumping. The fits, which assume thermal equilibrium and a pure sample of $m_j = 2$ atoms, yield the number (1.2×10^8), peak density (8×10^9 cm^{-3}), and temperature (1.3 mK) of the atoms.

A numerical approximation to Eq. (2) fits the data very well.

Our assumption for magnetic sublevel distribution means that the extracted temperatures are upper bounds, but one would expect the $m_j = 1$ level to be less populated. Due to the smaller magnetic moment, the trapping efficiency for $m_j = 1$ atoms decreases substantially as the MOT temperature increases, dropping by about a factor of 5 for a MOT temperature of 12 mK compared to only a factor of 2 for $m_j = 2$ atoms. Atoms with $m_j = 1$ can also be lost from the trap through spin-exchange collisions, which are typically rapid in ultracold gases. Calculated rates for spin-exchange collisions for alkali-metal atoms in magnetic traps are typically 10^{-11} cm^3/s, although they can approach 10^{-10} cm^3/s

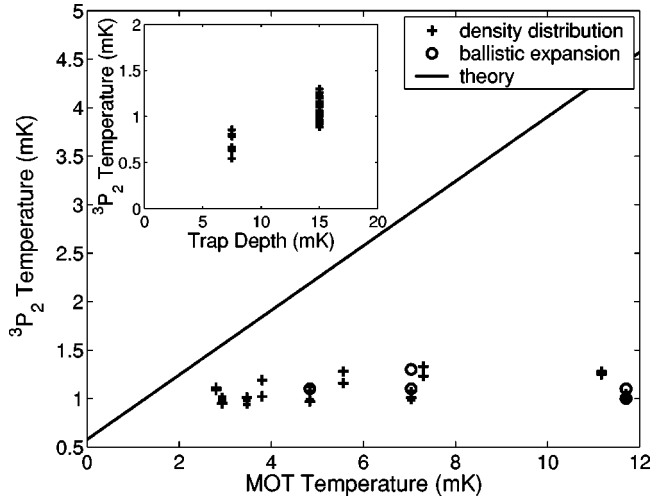

FIG. 5. The $^3P_2$ temperature is significantly lower than expected from a simple model that is described in the text. The inset shows that the temperature tracks the magnetic trap depth, as expected for evaporative cooling. The scatter of the temperature measurements is characteristic of our statistical uncertainty, and there is a scale uncertainty of 25% due to calibration of the imaging system. The magnetic trap depth is 15 mK for the main figure.

[21].

We have assumed thermal equilibrium in our analysis, but this is reasonable. Thermal equilibration would need to occur on less than a few hundred millisecond time scale. Using a recently calculated *s*-wave elastic scattering length for $^3P_2$ atoms of $a=6$ nm [22], the collision rate for identical atoms is $nv8\pi a^2 \approx 9\ \mathrm{s}^{-1}$ for $n=10^{10}\ \mathrm{cm}^{-3}$ and $v=\sqrt{2k_BT/M}=1$ m/s ($T=3$ mK).

The most interesting parameter obtained from the fits is the temperature, which is plotted in Fig. 5 as a function of MOT atom temperature. The values are significantly colder than what one would expect from a simple theory developed in Ref. [11] and plotted in the figure. The expected temperature is determined by assuming the kinetic energy and density distribution in the MOT are preserved as atoms decay to the metastable state. The $^3P_2$ potential-energy distribution is then given by the magnetic trap potential energy corresponding to the density distribution of the MOT. Actual $^3P_2$ atom temperatures cluster around 1 mK for a 15 mK trap depth, while the expected temperature approaches 4.5 mK for the hottest MOT conditions. We confirmed these measurements by determining the $^3P_2$ atom temperature from ballistic expansion velocities, as is done to measure the MOT temperature.

As shown in the inset of Fig. 5, the temperature decreases with decreasing trap depth as would be expected for evaporative cooling of the sample [23]. For this data, the magnetic trap depth is held constant during the entire load and hold time. Confirmation of this explanation could be achieved with the measurement of the collision cross section and thermalization rate in the trap. We plan to pursue experiments in that direction.

If evaporative cooling is working efficiently, it should be possible to use radio-frequency-induced forced evaporative cooling to further cool the sample and increase the density. Majorana spin flips [20] from trapped to untrapped magnetic sublevels at the zero of the quadrupole magnetic field will eventually limit the sample lifetime, but it will still be 10 s at 100 uK. For studies of quantum degeneracy, the sample would have to be transferred to a magnetic trap without a field zero or to an optical dipole trap. Straightforward improvement of our vacuum should yield atom numbers and densities an order of magnitude higher than currently attained, and should allow us to fully explore potential gains through evaporative cooling.

This research was supported by the Office for Naval Research, Research Corporation, Sloan Foundation, and U.S. Department of Energy, Office of Fusion Energy Sciences.

[1] C.W. Oates, F. Bondu, R.W. Fox, and L. Hollberg, Eur. Phys. J. D **7**, 449 (1999).
[2] H. Katori, T. Ido, Y. Isoya, and M. Kuwata-Gonokami, Phys. Rev. Lett. **82**, 1116 (1999).
[3] Y. Isoya and H. Katori, Phys. Rev. A **61**, 061403 (2000).
[4] M. Machholm, P.S. Julienne, and K. Suominen, Phys. Rev. A **64**, 033425 (2001).
[5] G. Zinner, T. Binnewies, F. Riehle, and E. Tiemann, Phys. Rev. Lett. **85**, 2292 (2000).
[6] T.P. Dinneen, K.R. Vogel, E. Arimondo, J.L. Hall, and A. Gallagher, Phys. Rev. A **59**, 1216 (1999).
[7] A. Derevianko, Phys. Rev. Lett. **87**, 023002 (2001).
[8] T. Loftus, J.R. Bochinski, and T.W. Mossberg, Phys. Rev. A **66**, 013411 (2002).
[9] H. Katori, T. Ido, Y. Isoya, and M. Kuwata-Gonokami, in *Atomic Physics XVII*, edited by E. Arimondo, P. DeNatale, and M. Inguscio, AIP Conf. Proc. No. 551 (AIP, Melville, NY, 2001), p. 382.
[10] T. Loftus, X. Y. Xu, J. L. Hall, A. Gallagher, and J. Ye (unpublished).
[11] J. Stuhler, P.O. Schmidt, S. Hensler, J. Werner, J. Mlynek, and T. Pfau, Phys. Rev. A **64**, 031405 (2001).
[12] W. Ketterle, K.B. Davis, M.A. Joffe, A. Martin, and D.E. Pritchard, Phys. Rev. Lett. **70**, 2253 (1993).
[13] J. Grunert and A. Hemmerich, Phys. Rev. A **65**, 041401 (2002).
[14] M.P. Robinson, B.L. Tolra, M.W. Noel, T.F. Gallagher, and P. Pillet, Phys. Rev. Lett. **85**, 4466 (2000).
[15] T.C. Killian, S. Kulin, S.D. Bergeson, L.A. Orozco, C. Orzel, and S.L. Rolston, Phys. Rev. Lett. **83**, 4776 (1999).
[16] J. Prodan, A. Migdall, W.D. Phillips, I. So, H. Metcalf, and J. Dalibard, Phys. Rev. Lett. **54**, 992 (1985).
[17] E.L. Raab, M. Prentiss, A. Cable, S. Chu, and D.E. Pritchard, Phys. Rev. Lett. **59**, 2631 (1987).
[18] M. Bode, I. Freitag, A. Tunnermann, and H. Welling, Opt. Lett. **22**, 1220 (1997).
[19] D.S. Weiss, E. Riis, Y. Shevy, P.J. Ungar, and S. Chu, J. Opt. Soc. Am. B **6**, 2072 (1989).
[20] A.L. Migdall, J.V. Prodan, W.D. Phillips, T.H. Bergeman, and H.J. Metcalf, Phys. Rev. Lett. **54**, 2596 (1985).
[21] S.J.J.M.F. Kokkelmans, H.M.J.M. Boesten, and B.J. Verhaar, Phys. Rev. A **55**, R1589 (1997).
[22] A. Derevianko, S.G. Porsev, S. Kotochigova, E. Tiesinga, and P.S. Julienne, e-print http://arXiv.org/abs/physics/0210076.
[23] W. Ketterle and N.J. van Druten, Adv. At., Mol., Opt. Phys. **37**, 181 (1996).